



FACILITY FORM 602

N65-32197

(ACCESSION NUMBER)	(THRU)
53	1
(PAGES)	(CODE)
CR 64451	09
(NASA CR OR TMX OR AD NUMBER)	(CATEGORY)

20023-FR1

FINAL REPORT

GG159 MINIATURE INTEGRATING GYRO
STERILIZATION EXPOSURE STUDIES AT 300°F

California Institute of Technology
Jet Propulsion Laboratory
Pasadena, California

JPL Contract No. 950769

NASA Contract NAS 7-100

10 June 1965

HONEYWELL *Aeronautical Division*

GPO PRICE \$ _____

CSFTI PRICE(S) \$ _____

Hard copy (HC) 3.00

Microfiche (MF) .50

FINAL REPORT

GG159 MINIATURE INTEGRATING GYRO
STERILIZATION EXPOSURE STUDIES AT 300°F

California Institute of Technology
Jet Propulsion Laboratory
Pasadena, California

JPL Contract No. 950769

Prepared by:

John K. Sarkinen
Development Engineer

Approved by:



R. G. Baldwin
Project Engineer
Inertial Components

Reviewed by:



Richard C. Amos
Program Administrator
Program Management



M. H. Riesgraf
Section Head
Inertial Components

Honeywell Inc.
Aeronautical Division
Minneapolis, Minnesota

CONTENTS

	Page	
SECTION I	INTRODUCTION	1
SECTION II	SUMMARY	3
	Stability and Random Drift	3
	Anisoelastic Drift	5
	Results of First Build	5
SECTION III	DEVELOPMENT STUDY	7
	Flotation	7
	Physical Specifications	8
	Gimbal Flotation Modifications	8
	Corrosion Tests	10
	Fluid Stability	13
	Adhesives	13
	O-Rings	13
	Balance Ring	15
	Gyro Case Stability	17
	Eutectic Alloy, Balance Pan	19
	Pump Assembly	19
	Hysteresis Ring	20
SECTION IV	EXPERIMENTAL GYRO	22
SECTION V	INITIAL GYRO PERFORMANCE	25
	Calibration and Adjustment Prior to Initial Tests	25
	Initial Tests	25
	Vibration	25
	Reference Drift	26
	Stabilization	26
	First Sterilization Cycle	27
	Second Sterilization Cycle	28
	Third Sterilization Cycle	29
	Preliminary Failure Analysis Following First 300°F Soak	29
	Preliminary Failure Analysis Following Second 300°F Soak	30
SECTION VI	FAILURE ANALYSIS AND DESIGN CHANGES	32
	Testing	32
	Corrective Action	35
SECTION VII	FINAL TEST RESULTS	39
	Calibration and Adjustments Prior to Initial Tests	39
	Test Results	39
	Vibration	39
	Stability and Random Drift	40
	Spinmotor Performance	47

ILLUSTRATIONS

Figure		Page
1	Gyro Balance Torque History	4
2	DGG159D1 G-Sensitive and G-Insensitive Torque History	6
3	Simplified Sketch of Modified Gimbal	9
4	Photograph of Materials Undergoing 200-Hour Immersion Test in Fluorolube Flotation Fluid	10
5	Hysteresis Ring with Venting Holes	21
6	Fluid Torque Stability of Experimental (Dummy) Gyro After 300°F Temperature Soaks, OAV	24
7	GG159D1 Anisoelastic and Attitude Angle Coefficients	26
8	GG159D1 Anisoelastic Coefficient Comparison	28
9	DGG159D1 G-Sensitive and G-Insensitive Torque History	31
10	Slot Bridge Deformation	33
11	Cross-Section View of Pump Stator and Windings	38
12	Attitude and Anisoelastic Drift Coefficient 5 g RMS	41
13	Anisoelastic Drift 5 g RMS Post + 300°F Cycle No. 1	42
14	Anisoelastic Drift Coefficient Post + 300°F Cycle No. 5	42
15	Gyro Balance Torque History	43
16	GG159 Gyro Outline Dimensions	44
17	GG159 Gyro Schematic Diagram	45

TABLES

Table		Page
1	DGG-159D-1 Performance Parameters, Goals, and Results	1
2	Corrosion Tests of Metals	11
3	Corrosion Tests of 7636 Flex-Lead Material	11
4	Bond Test Strengths	14
5	Corrosion Tests of O-Rings	16
6	Compression-Set of O-Ring Material	17
7	Dimensional Stability of 6061 Aluminum and 7075 Aluminum	18
8	Torque Stability of Experimental (Dummy) Gyro After 300°F Temperature Soaks. OAV	24
9	Measured Concentricities of Spinmotor Parts	33
10	Slot Bridge Concentricity	35
11	Slot Bridge Concentricities	36
12	Torque Shifts and Random Drift	43
13	Gyro Characteristics	44
14	Power Supply Requirements	46
15	Synchronous Speed Characteristics	-8

SECTION I
INTRODUCTION

This is the final report submitted in partial fulfillment of JPL Contract No. 950769. The program objectives were to conduct a material analysis and to implement design modifications to the Honeywell GG-159C to withstand five sterilization cycles of 300°F of 36 hours each.

The program goal of sterilization capability was met with the gyro designated the DGG-159D-1.

The performance goals were met in all areas except for torque shift during cycling. Performance parameters, goals, and actual results are shown in Table 1.

Table 1. DGG-159D-1 Performance Parameters, Goals and Results

Parameter	Goal	Actual
Mass unbalance (trimmed)	0.5 deg/hr/g	.18 deg/hr/g IA .55 deg/hr/g SA
Fixed torque (trimmed)	0.5 deg/hr	.15 deg/hr
Random Drift (4 hr. 1σ)		
OAV	.008 deg/hr	.003 deg/hr
IAV	.015 deg/hr	.003 deg/hr
Anisoelastic coefficient	.07 deg/hr/g ² max	.06 deg/hr/g ² max
Shifts due to 5 sterilization cycles		
Mass unbalance	.14 deg/hr max	0 IA .73 deg/hr/g SA
Fixed torques	.1 deg/hr	.53 deg/hr

This final report is arranged in chronological order of the work sequence.

- Development Study
- Experimental Gyro
- Initial Gyro Test Results
- Failure Analysis and Corrective Action
- Final Gyro Test Results

The Development Study was an extensive study of materials and components exposed to a 300°F environment for a prolonged period of time. Decisions on the final configuration were made based on the results of this work.

An experimental dummy gyro was assembled and tested to determine effects of miscellaneous changes which could not be evaluated at a piece-part level.

The actual gyro build and testing proceeded smoothly up to the third sterilization cycle, when the spinmotor failed to start. A preliminary failure analysis was made at the gyro level. Testing showed the load torque at stall had increased but the exact cause was not determined.

The gyro was torn down and the problem area was identified in the stator assembly. Design modifications were made and evaluated to assure that the problem was solved.

The gyro was then rebuilt and evaluation of the unit was performed through five sterilization cycles.

SECTION II SUMMARY

The ultimate goal of the contract was the development of a gyro which would withstand sterilization cycling. For this reason the results of the development program and the miscellaneous problem areas encountered are covered in their respective sections.

Performance of the final gyro assembly is summarized below. Although all of the performance goals were not met, the gyro did demonstrate sterilization capability and could be used in missions requiring sterilization capability.

STABILITY AND RANDOM DRIFT

The g-sensitive and non-g-sensitive torques and the random drift of the gyro were determined initially and after each sterilization cycle. A summary of the torque shifts and random drifts is tabulated in Figure 1.

The torque shifts during sterilization cycling were not excessive, except for the first cycle. It is normal for these torques to take a stabilizing shift on the first temperature cycle after build. These shifts can be minimized by an initial temperature cycle before trimming and proceeding to the sterilization cycling. This is demonstrated by the results of the first build. The g-sensitive and non-g-sensitive torques did not take the large shift on the first sterilization cycle. This unit was cycled prior to sterilization cycling.

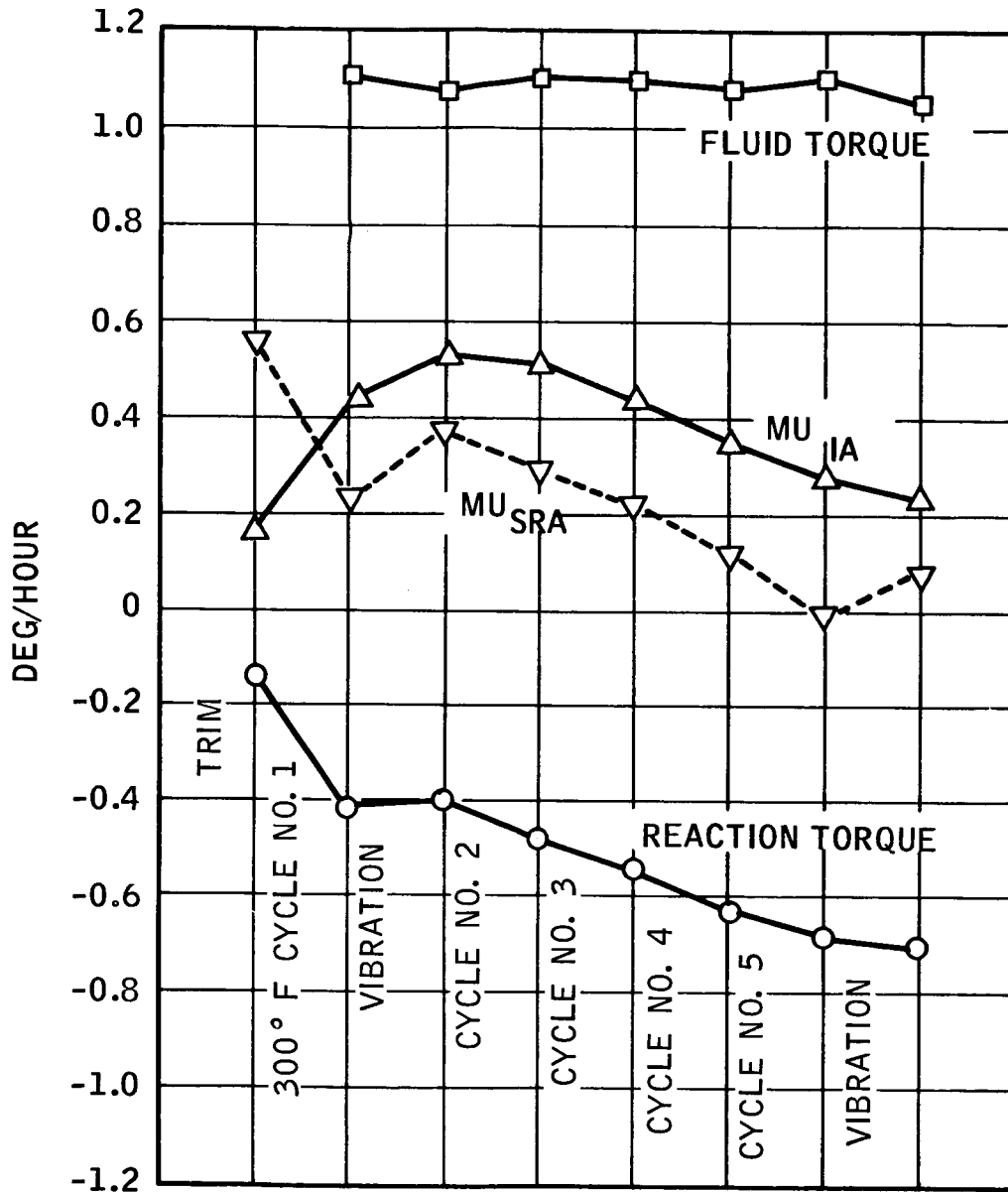


Figure 1. Gyro Balance Torque History

ANISOELASTIC DRIFT

The measured anisoelastic drift was 0.06 deg/hr/g² maximum. An average value for the frequency spectrum of 20-2000 cps is about 0.03 deg/hr/g². These values are below the goal of 0.07 deg/hr/g². These performance areas are the highlights of the testing. Gyro parameters and miscellaneous test data are covered in Section VII.

RESULTS OF FIRST BUILD

The balance torque history of the first gyro build is shown in Figure 2. The large shifts which occurred after the third sterilization cycle are the result of mechanical inputs to the gyro in an attempt to start the spinmotor.

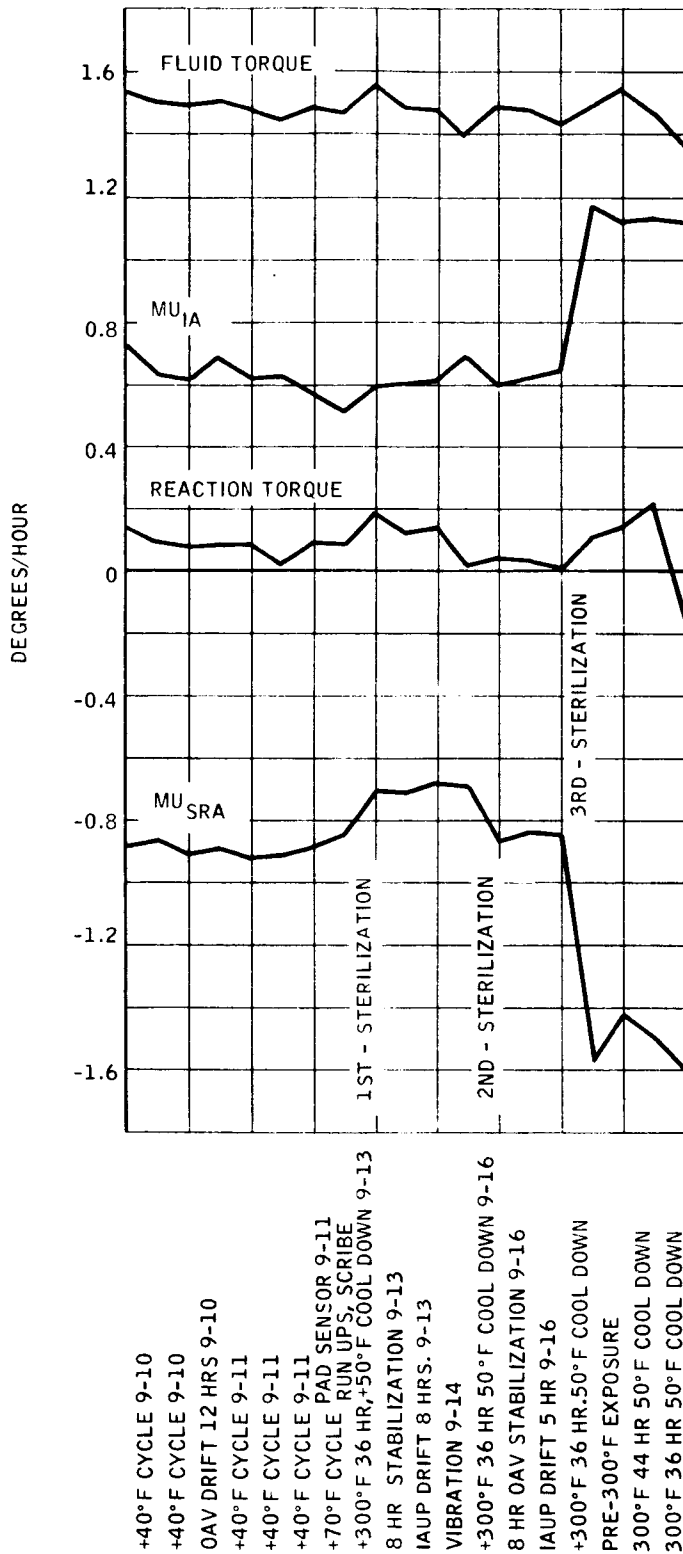


Figure 2. DGG159D1 G-Sensitive and G-Insensitive Torque History

SECTION III DEVELOPMENT STUDY

The development study was performed to determine which materials and subassemblies would withstand the prolonged exposure to 300°F during sterilization cycling.

The areas of investigation included:

- Gimbal Flotation, Fluid and Gimbal Changes
- Adhesives
- O-Rings
- Balance Rings
- Gyro Case Stability
- Eutectic Alloy-Balance Pan
- Pump Assembly
- Hysteresis Ring

FLOTATION

A change in the normal Bromolube flotation fluid used in the GG-159C was required for sterilization capability because of the chemical breakdown temperature (285°F) of Bromolube with resulting corrosion tendencies. The change of fluid initiated four areas of investigation:

- The complete physical specifications of Fluorolube, such as pour point, viscosity, cloud point, fracture point and volatility, had to be determined.

- Because of Fluorolube's lower density, the gimbal had to be modified to assure flotation.
- Possible effects of corrosion on the materials which would be in contact with the flotation fluid had to be investigated.
- Whether the fluid's viscosity would remain stable under sterilization cycling had to be discerned.

Physical Specifications

The physical characteristics of the fluid were determined and are covered by an internal specification.

Gimbal Flotation Modifications

The major design modification was due to the change from Bromolube to Fluorolube, resulting in lower buoyancy. The need to increase the gimbal volume or decrease the gimbal weight was due to the lower density of the Fluorolube.

A detailed design layout of the gimbal and adjacent gyro components revealed that the best way to reduce gimbal weight was to remove the "fork" which connects the motor shaft to the gimbal cup end. This was done, and the shaft is now mounted directly to the cylindrical wall (see Figure 3). The modified gimbal is arranged so that the flex-lead end of the gimbal and the cylindrical wall are one piece and an end plate (near the hydrostatic pump end) closes the gimbal. Minor changes made in the wall thickness lowered the gimbal weight. Shaft mounting and gimbal sealing arrangements are almost identical to previous methods.

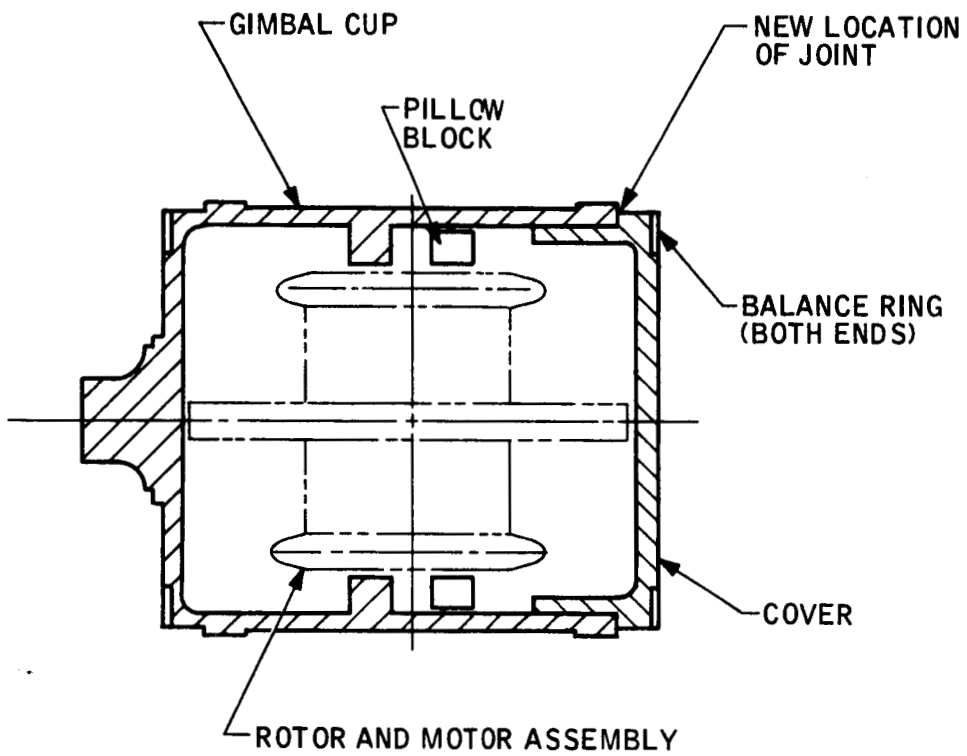


Figure 3. Simplified Sketch of Modified Gimbal

Primary advantage of this approach is the weight reduction within the gimbal, removing the need to modify any of the adjacent components. A second advantage is the more direct method of supporting the shaft; (i. e., from the fluid to the wall to the shaft) instead of from the fluid to the wall and then through the cantilever fork to the shaft. G^2 drift of the gyro was also improved.

Corrosion Tests

Samples of the following materials were immersed in flotation fluid and checked for weight change and discoloration after more than 200 hours and 1000 hours at 300°F: brass, 303 stainless, 52100 bearing steel, Hipernik Armco iron (tin-plated), plain Armco iron and chromatic aluminum.

Tables 2 and 3 list the results of corrosion specimens immersed in Fluorolube. In Table 2, only brass, Hipernik and plain Armco-iron show a slight tarnish. This is not harmful to gyro operation as long as the fluid remains clear. The weight changes are insignificant; that is, they do not affect gyro stability.

Table 3 shows the flex-lead results. The 22 percent weight change after 200 hours appears to be extremely high. However, this in itself is not believed to be detrimental, since the fluid remains unaffected (remains clear). The accuracy of this measurement is somewhat questionable in view of the much lower weight change after 1000 hours and also the very small quantities involved. Therefore, a change in material is not considered necessary. Figure 4 is a photo of some of the materials during the test.

Spectrographic analysis was performed on the fluid to determine if the material had contaminated the fluid. No foreign materials were detected.

Table 2. Corrosion Tests of Metals

Material Immersed in Fluid	200-Hour Test		1000-Hour Test	
	Corrosion	Weight Change	Corrosion	Weight Change
Fluorolube by itself	No change in color or clarity	-	No change in color or clarity	-
Brass (6521)	Slight tarnish	0.005% gain	Slight tarnish	0.01% gain
303 Stainless (6513)	No sign	0.003% gain	No sign	0.01% gain
52100 Bearing Steel	No sign	0.1% loss	Light film	0.01% loss
Hipernik (6536)	Very slight tarnish	0.002% gain	Slight tarnish	0.002% gain
Armco-Iron (tin plated)	No sign	0.01% gain	No sign	0.01% gain
Armco-Iron (6663)	One side showed rust-like film	0.005% gain	Slight tarnish	0.002% gain
Chromate Aluminum	No sign	0.02% loss	No sign	0.003% loss
Infrared Analysis: Spectrographic Analysis:	No organics after 200 hours and 1000 hours Negative			

Table 3. Corrosion Tests of 7636 Flex-Lead Material

Test	Test Conditions	
	200 Hours	1000 Hours
Weight change	22% gain	1.2% gain
Appearance of fluid	No change in color or clarity	No change in color or clarity
Appearance of flex-leads	No sign of corrosion	No sign of corrosion
Infrared analysis	No organics	No organics
Spectrographic analysis	Negative	Negative

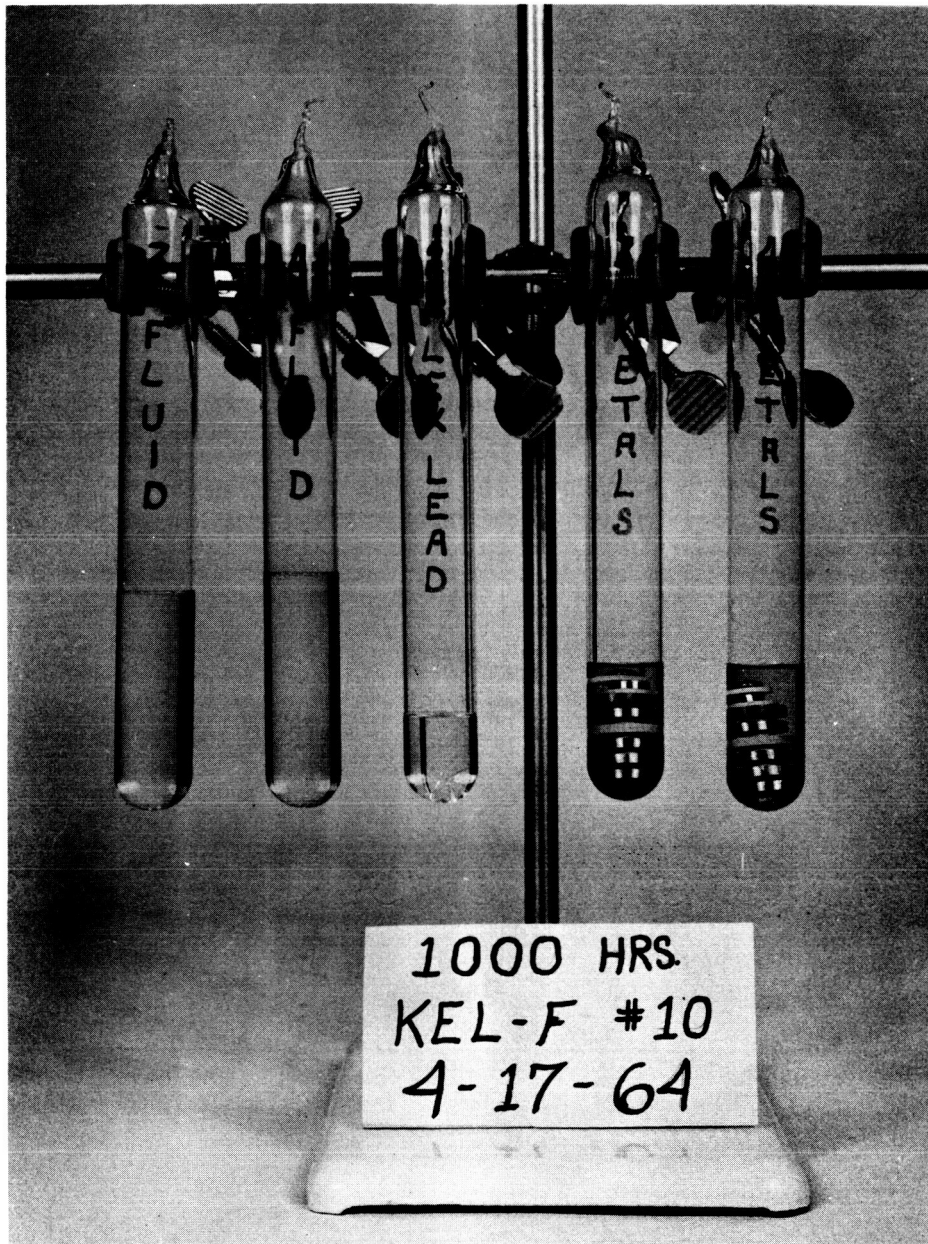


Figure 4. Photograph of Materials Undergoing 200-Hour Immersion Test in Fluorolube Flotation Fluid

Fluid Stability

The viscosity of the Fluorolube was checked before and after more than 200 hours at 300°F. The viscosity change was insignificant (0.6 percent); therefore the gyro gain will not be affected.

ADHESIVES

A large group of materials in question were those bonded with epoxy adhesives. To assure that no problems would exist with the epoxies, various samples of materials and epoxy combinations were tested to determine the effects of sterilization cycling. The simulated joint configurations were run through 10 sterilization cycles, and then the tensile strength of the joint was measured.

Table 4 summarizes the bond test results of the adhesives tests. The last column in the table lists values from previous tests after five thermal cycles from 200°F to -65°F. The higher values noted after sterilization cycling may be caused by a diffusion of the various materials with resulting increase in bonding strength.

In general, an epoxy bond strength of 1000 psi will provide an adequate joint. There are exceptions where the epoxy is used as a filler material such as in the Alnico SMRD magnets in the rotor.

O-RINGS

Although no O-Rings are used as hermetic seals, an O-ring is used to separate fluid flow within the gyro. Therefore, a particularly important test in the series in the O-ring material, which must be compatible with the fluid at high temperature, but must also have a high degree of resistance to compression set at 300°F. After reviewing O-ring literature and contacting the suppliers, three silicone rubber materials were purchased. These materials differ in the curing agents used and in the curing temperature.

Table 4. Bond Test Strengths

Test Environment: 10 cycles of 300°F for 36 hours
and room temperature

Materials Bonded	Bonding Agent	Tensile Strength (psi)	Previously Known Strength
Kovar - Lucalox	6293G	2235	1490
Zirconium - Lucalox	6293G	2495	370
Lucalox - 2-micro-finish Lucalox	6293G	2665	
Lucalox - Lucalox	6293G	2360	1510
Simonds No. 81 - Lucalox	7553A	2900	1500
Hypernik - Lucalox	6293G	1285	235
Alnico V - Lucalox	6293N	970	
Zirconium - A203 Ceramic	6293F	5340	
Zirconium - A203 Ceramic	6293J	3690	
Zirconium - A203 Ceramic	6293G	4185	
Tungsten - A203 Ceramic	6293F	5980	
Tungsten - Lucalox	6293G	4210	2460
A203 Ceramic - A203 Ceramic	6293F	3735	

Table 5 shows the corrosion data of O-ring materials. However, this information should be considered along with the compression-set data of Table 6. Several samples crumbled during the hardness test, after 1000 hours submersion in Fluorolube. The spectrographic analysis of these samples also showed a trace of silicone in the fluid. This means that the fluid is corroding the rubber. However, the function of the fluid would be significantly impaired if the impurities were to clog the hydrostatic support gaps, the filter, or any other small passage. Since the fluid remained clear (though amber in color), the impurities are not believed to affect fluid consistency.

Some reflection on the required service of this O-ring leads to the conclusion that, for several reasons, the lowest compression-set should govern the choice. For instance, much of the O-ring surface will be in contact with metal rather than fluid. This will probably reduce the rate of embrittlement. Also, it is important that the O-ring maintain contact with mating surfaces, and for this, the low compression-set rating is desirable. It should further be noted that the length of time in which the material was exposed to high temperature was extreme. For the anticipated gyro tests, the total exposure period is considerably less than 1000 hours where embrittlement is not evident (see hardness change after 200 hours). The conclusion is that type A710B(S2-096) is the material to be used.

BALANCE RING

Tests results showed that "Heavimet" material used in the gimbal balance rings absorb Bromolube unless impregnated with an epoxy. The effect of any assymetrical weight gain of the balance ring will reflect as a change in mass unbalance on the gimbal, resulting in a degraded performance of the unit. Substitution of tantalum for Heavimet improved the weight change, and impregnated tantalum showed still less weight change. The over-all improvement from Heavimet to impregnated tantalum is a factor of 100. This change was implemented on the GG159D.

Table 5. Corrosion Tests of O-Rings

Material	Test Conditions	
	200 Hours	1000 Hours
Red O-Ring Stock A710-A(S2-096) Weight change Thickness change Hardness change Fluid appearance Infrared analysis Spectrographic analysis	32% gain 9% greater 16% loss No change in color or clarity	30% gain 1.9% loss No reading - crumbled Clear - amber in color Large trace silicone Large trace silicone
Red O-Ring Stock A710B(S2-096) Weight change Thickness change Hardness change Fluid appearance Infrared analysis Spectrographic analysis	30% gain 10% gain 18% loss No change in color or clarity	36% gain 3% loss No. 1: 13% greater No. 2: Crumbled Clear - amber in color Large trace silicone Large trace silicone
White O-Ring Stock 610A(LS-63) Weight change Thickness change Hardness change Fluid appearance Infrared Spectrographic	8% gain 1.3% gain 2% loss No change in color or clarity No organics Small trace silicone	7.8% gain 2.7% gain 28% loss Clear - very light amber color - -

Table 6. Compression-Set of O-Ring Material

Test Environment: Specimen immersed in fluid,
under load and subjected to 10
cycles of 300°F for 36 hours each

Material	Percent of Compression-Set After	
	7 Cycles	10 Cycles
A710A	11	18
A710B	4	7.7
LS63	41	49

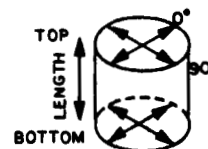
GYRO CASE STABILITY

The material used in the GG-159C is 7075-T6 aluminum alloy, which age hardens at 250°F. Sample gyro cases of this material and 6061 aluminum alloy, with and without stress relief, were sterilization cycled and measured at significant places before and after cycling.

A comparison of the two materials in Table 7 shows 6061 aluminum is more stable than 7075 aluminum. The latter shrank, almost without exception, an amount varying from 100 to 1000 microns, as compared with a random change (shrinkage or expansion) for 6061 aluminum of between 10 to 100 or 200 microns. This amounts to approximately an order of magnitude improvement. There is no evident improvement due to stress relieving. However, a continuous soak at a lower temperature (200°F) resulted in small, random changes in either material.

Significance of the small, random changes in 6061 was evaluated in the dummy unit and the final assembly. The fluid torque stability showed that these small random changes did not adversely affect gyro performance.

Table 7. Dimensional Stability of 6061 Aluminum and 7075 Aluminum (in microinches)



Test Environment (10 cycles of 300°F to room temperature)	Sample	Top		Bottom		Length	
		0°	90°	0°	90°	0°	90°
6061 Aluminum							
Stress-relieved	1	-130	-110	-220	+ 50	+ 170	+ 190
	2	+ 20	+ 20	+ 10	+ 10	+ 70	+ 70
	3	-120	+ 70	-190	- 40	+ 75	+ 25
	4	+ 30	+ 40	+180	+ 60	- 30	- 20
	5	+ 10	- 20	0	- 80	+ 20	- 30
Not stress-relieved	6	+160	- 70	+ 10	- 70	+ 20	+ 40
	7	- 70	- 80	- 30	-210	+ 30	+ 20
	8	- 10	-120	- 30	- 30	- 110	- 170
	9	- 50	- 20	- 50	- 40	- 40	+ 40
	10	- 60	- 80	-170	- 50	- 20	- 10
7075 Aluminum							
Stress-relieved	17	-130	-260	-580	-240	- 360	- 250
	18	-300	-320	-260	-260	- 430	- 480
	19	-340	-440	-360	-390	- 420	- 580
	20	-610	-750	-670	-890	-1090	- 910
	21	-540	-330	-390	-220	- 430	- 500
Not stress-relieved	22	-500	-270	-350	-300	- 480	- 480
	23	-600	-690	-720	-750	- 710	-1030
	24	-710	-650	-830	-850	- 820	- 800
	25	-710	-520	-790	-510	- 970	-1050
	26	-530	-690	-550	-760	- 990	- 990

EUTECTIC ALLOY, BALANCE PAN

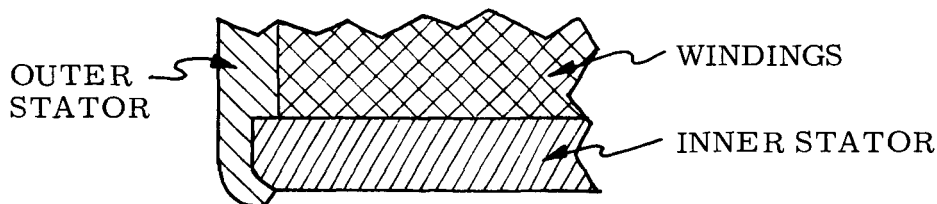
The melting point of the alloy normally used in the GG-159C is below the sterilization temperature of the gyro. A new alloy was required, and the following were used as goals.

- Ideal melting point - 325°F
- Freezing range - 10°F

A solder with a composition of 63 percent tin and 37 percent lead was tested for melting range and wetting capability on the conventional balance pan. Melting range was from 356°F to 361°F, well under the 10°F maximum range set as a goal. The melting temperature was somewhat higher than the ideal 325°F; however, there were no difficulties in supplying the extra heat energy for melting. This factor actually increases the safety margin of the eutectic during sterilization cycling. Wetting of the alloy to the balance pan plating appeared adequate. Several pans were cycled for possible blistering of the plating and magnetic properties changes. Both tests were negative.

PUMP ASSEMBLY

During early tests on the pump assembly a weak epoxy joint caused the stator to "pop out" during the 300°F temperature soaks. The parts were modified so that the outer wall could be rolled over to effect a mechanical lock between the inner and outer stators (see sketch below). Assemblies of this configuration successfully withstood the 300°F temperature cycling.



HYSTERESIS RING

The magnetic stability of the hysteresis ring was another area of concern. The coefficient of thermal expansion mismatch between the hysteresis ring and rotor materials is sufficient to induce high stresses in the hysteresis ring if the ring is mounted in a normal manner.

Two methods employing shrink fits were investigated. The one chosen consisted of a ring with a thin shrink fit band at each end and a means of allowing for axial differential expansion (see Figure 5). The advantages of this design are the double support of the ring and the localized contact area which reduces axial slippage. The ring's magnetic properties in a ceramic rotor showed very little change after shrink-fitting, and again after thermal cycling.

Radial holes were drilled to allow flushing and venting the narrow cavity between ring and rotor. This is important, since even small amount of trapped substances, such as cutting oils or soda blasting grit, could cause bearing failure. Several motor and bearing tests were conducted in the subassembly stage to assure performance before gyro assembly.

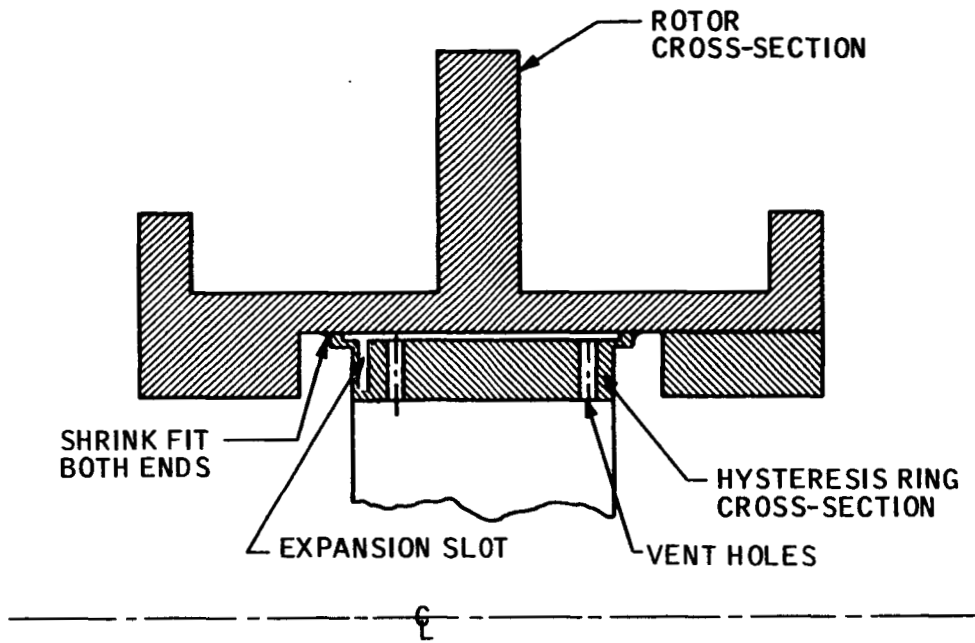


Figure 5. Hysteresis Ring with Venting Holes

SECTION IV EXPERIMENTAL GYRO

The experimental unit was fabricated for the following reasons:

- To pre-cycle the subassemblies and to test them for outright failure
- To test the stability of the reaction torque
- To uncover any complication during assembly and testing due to non-compatibility of materials, filling technique, or geometric changes at high temperature.

This gyro has yielded significant results in all three areas. The subassemblies were cycled and checked as follows:

- The header assembly was checked for continuity, leaks, and dielectric breakdown at 500 volts. There was no failure.
- The hydrostatic pump was checked for continuity. There was no failure. This pump had the modified interlock preventing the stator from coming apart.
- The case was checked for dimensional stability. The case material was a different grade of aluminum, as described in the material study. The shrinkage of this case was small and compared with the results of the study.
- The gimbal was checked for leaks. The leak rate was below the allowable rate for a hermetic seal.

The motor in this model was replaced by two zirconium dummy weights. The other significant substitutions were: Fluorolube for Bromolube, and high-temperature cements and solder for their conventional counterparts. In all other respects, the gyro is a GG159C.

The gyro was tested on the test stand for reaction torques between successive sterilization cycles. The results are listed in Table 8. The fluid torque is listed in the last column, and is also plotted in Figure 6. The shifts are random, but quite small ($\sim 0.15^\circ/\text{hour}$ spread). This is an important result as it reflects the relative stability of the case and gimbal material near the fluid gaps. Furthermore, the low fluid torque is due to the reduced fluid flow at the lower pump frequency of 12.5 cps. On the other hand, the flex-lead torque shows large random shifts. This is believed to be due to the low forming temperature (300°F) used on the present flex-leads. In effect, the flex-leads are probably being reformed during each sterilization cycle, wherever the gimbal may happen to be oriented. To confirm this theory, a series of tests was begun in which the gyro was held at a known angular position during high temperature exposure. This was implemented simply by servoing the gimbal and using the case heater during the sterilization cycle. These tests showed a flex-lead torque shift of only $0.15^\circ/\text{hour}$, a marked improvement.

Silver-copper flex-leads were used in the final unit; this material formed at 450°F , thus minimizing excessive torque shifts at lower temperatures.

Table 8. Torque Stability of Experimental (Dummy) Gyro After 300°F Temperature Soaks, OAV

Ref. Run No.	Time of 300°F Soak (hrs)	Total Reaction Torque (°/hr)	Flex Lead Torque (°/hr)	Fluid Torque (°/hr)
0	0	-5.54	-5.03	-0.51
1	20	-3.92	-3.54	-0.38
2	39	-1.47	-0.99	-0.48
3	21	-0.78	-0.28	-0.50
4	23	+0.04	+0.47	-0.43
5	21	-0.34	+0.13	-0.47

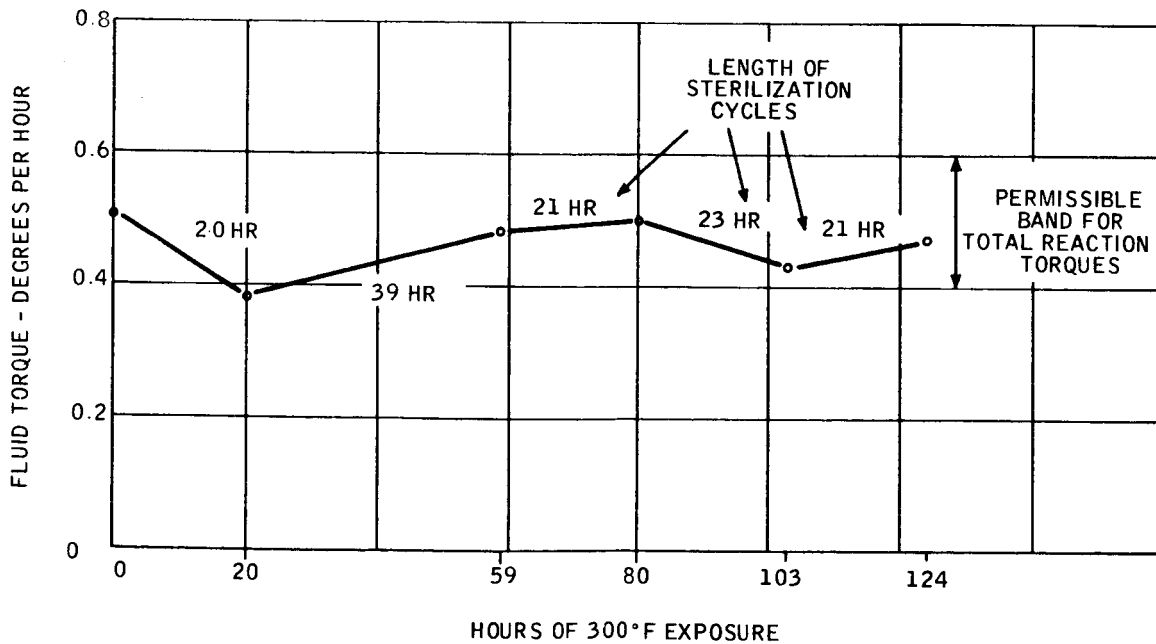


Figure 6. Fluid Torque Stability of Experimental (Dummy) Gyro After 300°F Temperature Soaks, OAV

SECTION V INITIAL GYRO PERFORMANCE

All of the gyro subassemblies were sterilization-cycled prior to final assembly. After final assembly, the gyro was submitted to evaluation. The results of the evaluation, including the preliminary failure analysis, are tabulated below in chronological order.

CALIBRATION AND ADJUSTMENT PRIOR TO INITIAL TESTS

The resistance of the temperature sensing element was rechecked by placing the gyro in a 185°F-water bath. The sensor was then series padded to 780 ohms at 185°F.

The hydrostatic suspension pump was operated at various frequencies from 10 to 110 cps one-half wave rectification. Twenty cps was selected as the optimum to provide adequate gimbal support with low-fluid torque.

The fixed torque was compensated to 0.09 deg/hr.

Gimbal mass unbalance was adjusted to $-0.58 \text{ deg/hr MU}_{\text{SRA}}$ and $0.53 \text{ deg/hr MU}_{\text{IA}}$.

INITIAL TESTS

Vibration

The gyro was vibrated and the anisoelastic coefficient determined and plotted. Attitude angle coefficients were determined and plotted (see Figure 7 for results).

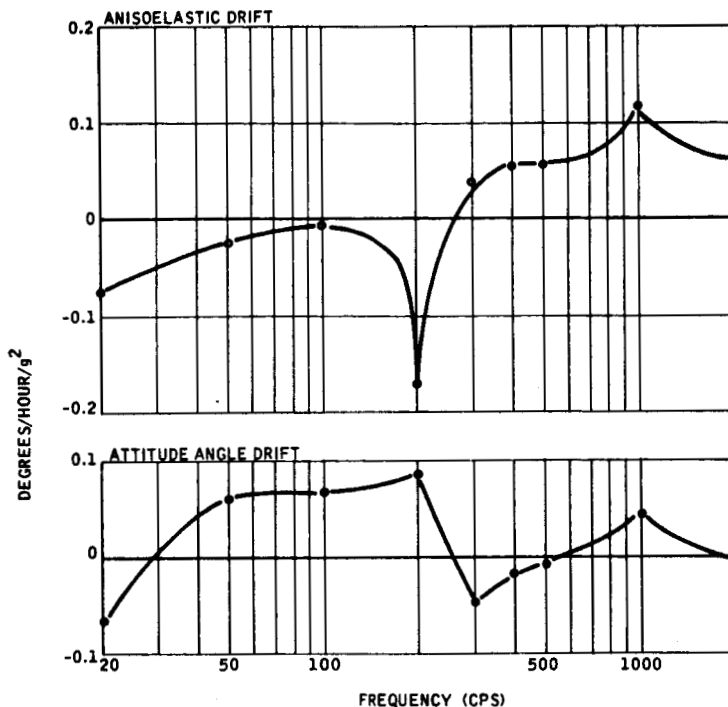


Figure 7. GG159D1 Anisoelastic and Attitude Angle Coefficients

Reference Drift

Random drift testing was accomplished with the following results:

- OAV 0.0051 deg/hr (1 σ for 4 hours)
- IAV 0.0039 deg/hr (1 σ for 4 hours)

Stabilization

The gyro was cycled three times from operating temperature to 40°F to stabilize gravity sensitive and gravity insensitivity torques. A set of reference readings were taken (six position test) prior to the first sterilization cycle.

FIRST STERILIZATION CYCLE

The gyro was removed from the dividing head at a temperature of 185°F and placed in an oven preheated to 185°F. The oven control was then reset to 300°F. After 36 hours at 300°F, the gyro was cooled to 50°F in four equal steps during a 2-hour period; i. e., the oven was first reset to 240°F, one half hour it was reset to 180°F, etc.

After the hot soak, the gyro was energized and allowed to stabilize for eight hours.

The following shifts took place during the sterilization cycle:

- Mass unbalance (input axis) = +0.08 deg/hr
- Mass unbalance (spin axis) = +0.14 deg/hr
- Reaction torque = +0.04 deg/hr

Random drift after first sterilization cycle:

- OAV (1σ) = 0.0091 deg/hr (4-hour period)
- IAV (1σ) = 0.0042 deg/hr (4-hour period)

The gyro was vibrated again and anisoelastic coefficients were determined and plotted. (See Figure 8 for before and after sterilization comparison.)

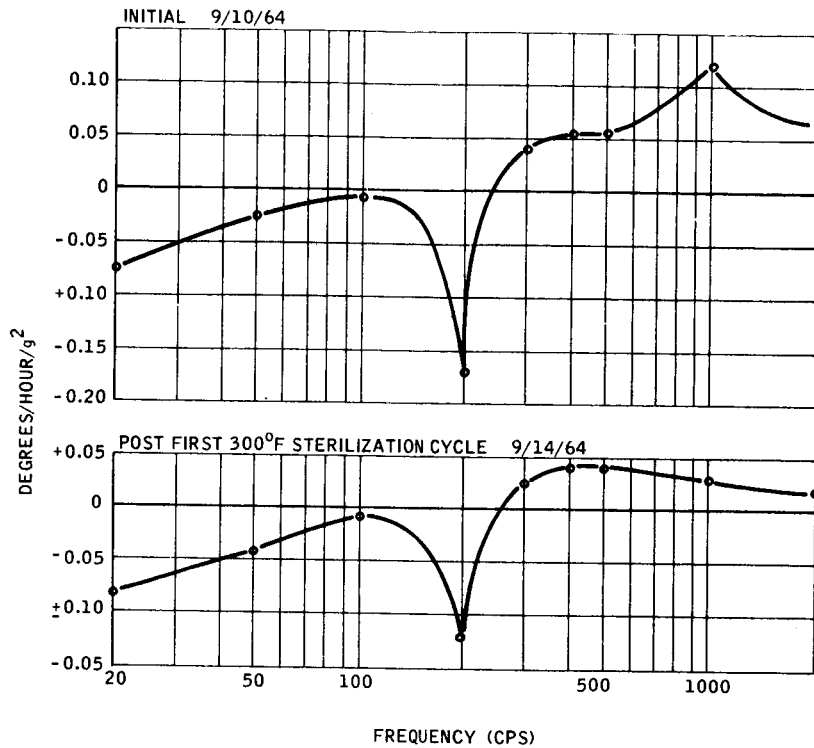


Figure 8. GG159D1 Anisoelectric Coefficient Comparison

SECOND STERILIZATION CYCLE

The gyro was subjected to a second sterilization cycle according to the same procedure used on the first cycle.

The following shifts took place during the sterilization cycle:

- $MU_{IA} = -0.07 \text{ deg/hr}$
- $MU_{SA} = -0.15 \text{ deg/hr}$
- $RT = +0.012 \text{ deg/hr}$

Random drift after second sterilization cycle was:

- OAV (1σ) = 0.0052 deg/hr (4-hour period)
- IAV (1σ) = 0.0076 deg/hr (4-hour period)

THIRD STERILIZATION CYCLE

The gyro was subjected to a third sterilization cycle according to the same procedure used on the first and second cycles. The gyro failed to start when first energized after the third sterilization cycle. After twisting the gyro about the spin axis the motor started.

The following shifts took place during the sterilization cycle and subsequent starting attempts:

- $MU_{IA} = +0.531$ deg/hr
- $MU_{SA} = -0.740$ deg/hr
- RT = +0.093 deg/hr

At this time JPL was called and advised of the starting failure. JPL concurred with the recommended preliminary failure analysis.

PRELIMINARY FAILURE ANALYSIS FOLLOWING FIRST 300°F SOAK

The gyro was subjected to 44 hours of the 300°F soak. The spinmotor again failed to start with the gyro at room ambient. The motor started when the gyro temperature was near 185°F.

The following shifts took place during the high temperature cycle:

- $MU_{IA} = +0.008 \text{ deg/hr}$
- $MU_{SA} = -0.071 \text{ deg/hr}$
- $RT = +0.076 \text{ deg/hr}$

Random drift OAV was 0.0039 deg/hr (1σ 4-hour period).

PRELIMINARY FAILURE ANALYSIS FOLLOWING SECOND 300°F SOAK

The gyro was soaked at 300°F for 36 hours. Again the spinmotor failed to start immediately. However, the spinmotor started after it was soaked at 197°F for 2-1/2 hours.

The following shifts took place during the high temperature cycle:

- $MU_{IA} = -0.015 \text{ deg/hr}$
- $MU_{SA} = -0.117 \text{ deg/hr}$
- $RT = -0.367 \text{ deg/hr}$

G-sensitive and G-insensitive torque history is plotted in Figure 9.

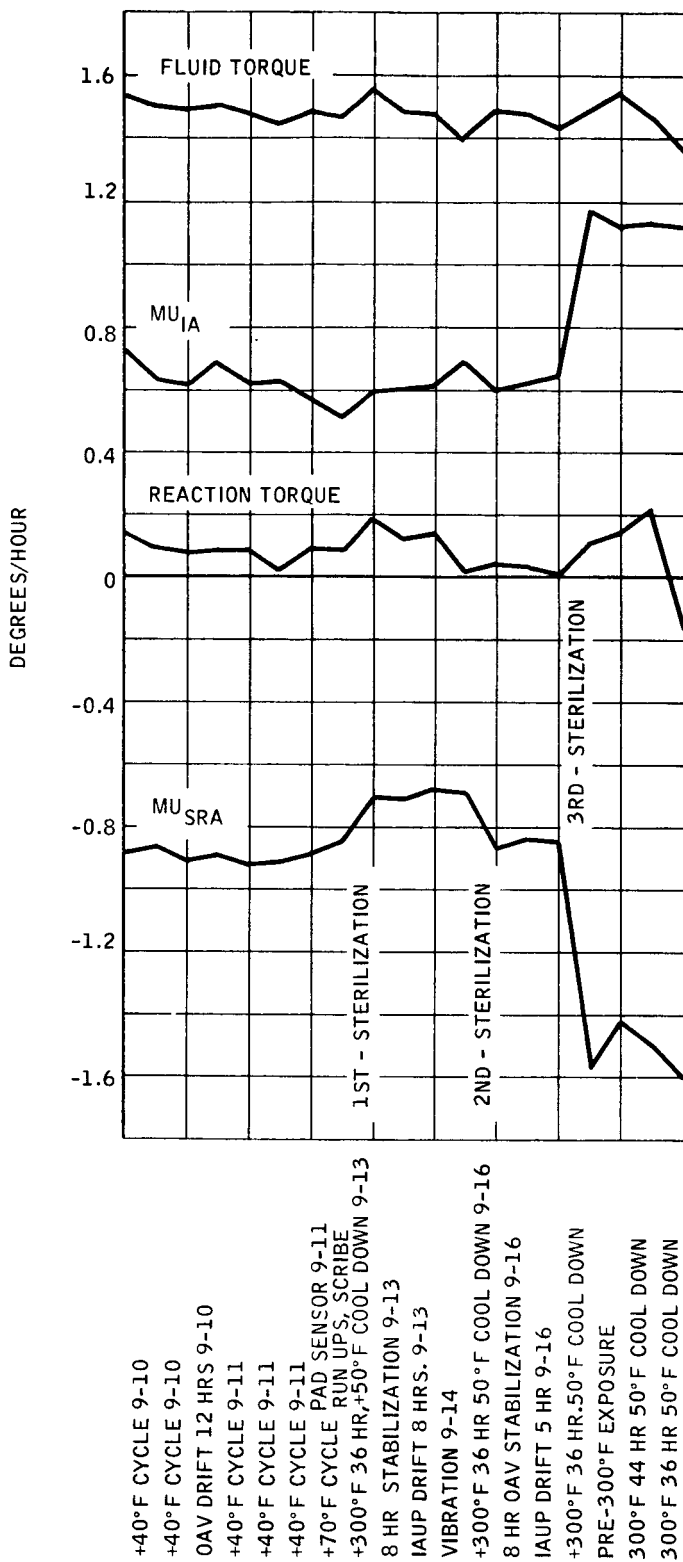


Figure 9. DGG159D1 G-Sensitive and G-Insensitive Torque History

SECTION VI
FAILURE ANALYSIS AND DESIGN CHANGES

TESTING

After the spinmotor failure, various tests were run on the gyro in an attempt to determine why the spinmotor would not start.

The results of the tests indicated the following:

- There was no apparent lube seepage into the gimbal
- The gimbal fill gas was of the correct viscosity
- The gas-bearing surfaces were contaminated with a temperature-sensitive contaminant.

Teardown of the gyro and gimbal assembly verified the first two conclusions. The third was erroneous. The test data indicated an increased load torque at stall conditions. The load torque increase was caused by a contact between the hysteresis ring and the stator slot bridge.

When the spinmotor was disassembled, wear areas were found on the stator slot bridge. These areas immediately pinpointed a problem as the manufactured clearance between the slot bridge and the hysteresis ring is 0.001 ± 0.0001 inch. The rotor and shaft assemblies were inspected to determine which elements were not in their proper position. Indi-ron traces were taken of both assemblies, with results as indicated in Table 9.

Measurement of the diameter of the slot bridge at the wear areas and at the center of the slot bridge showed that the diameter at the wear areas was from 0.0008 to 0.001 greater than at the center (see Figure 10).

Table 9. Measured Concentricities of Spinmotor Parts

Item	Measured Concentricity	Print Tolerances
Rotor Journal Bearings	0.000008	0.000010
Hysteresis Ring	0.000030	0.000100
Shaft Journal Bearings	0.000010	0.000010
Slot Bridge	0.000400	0.000100

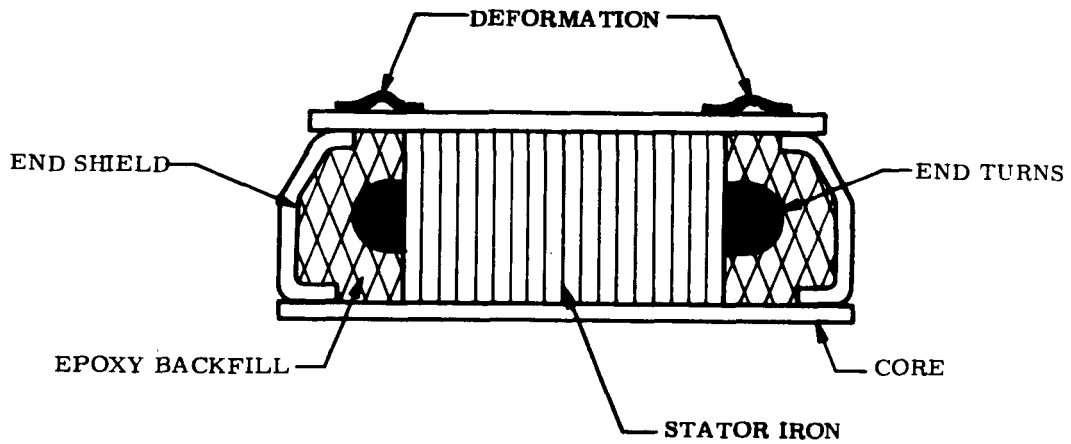


Figure 10. Slot Bridge Deformation

A stress analysis was run on the stator assembly to pinpoint the cause of the deformation. The analysis showed that the axial and radial stresses in the slot bridge material exceed the yield stress. Stresses in the slot bridge for a 230°F temperature excursion are:

Axial stress	65,000 psi
Radial	38,000 psi
Yield stress	22,000 psi

These high stresses are caused by two factors: (1) The epoxy fill between the end shield, and (2) the thermal coefficient mismatch between the hypernik slot bridge and the stainless steel end shield.

The backup shaft and stator assembly from the original build had been processed through the assembly stage, but was not ground.

This assembly was processed to determine the extent of slot bridge deformation on a second assembly. The processing was as follows:

The slot bridge was ground to within 0.0008 inch of the correct size. The assembly was then cycled to 300°F for one hour and an additional 0.004 inch of material was removed. (This interim temperature cycling and a final skin cut on the slot bridge is normal processing for this type assembly.) The shaft assembly was then cycled as follows: 300°F, 36 hours minimum to 40°F, 1 hour minimum. This cycle was repeated for a total of three cycles. The slot bridge concentricity was measured at interim stages with results as tabulated in Table 10.

Table 10. Slot Bridge Concentricity

Processing Stage	Top	Middle	Bottom
After Initial Grinding	0.000030	0.000020	0.000015
One hour, 300°F soak	0.000085	0.000100	0.000260
Second Grind	0.000040	0.000035	0.000045
First Sterilization Cycle	0.000100	0.000090	0.000100
Third Sterilization Cycle	0.000100	0.000220	0.000240

The results of this testing show that the slot bridge does not assume a stable position after the first cycle. A slight deformation can occur on additive cycles as shown in Table 10. This mode of deformation explains why the failure on the original unit did not appear until several sterilization cycles had been completed.

CORRECTIVE ACTION

To eliminate slot bridge deformation, the stress levels in the slot bridge must be well under the yield stress. Alternate materials with a lower coefficient of thermal expansion (CTE) must be used. The 400 series stainless steels would be a good choice, except for their magnetic properties. If a magnetic stainless steel is used, some of the air gap flux will be shunted through the slot bridge material. Typically, this will be about a 10 percent reduction in the developed torque per watt of input power. While this is not desirable, it would not eliminate use of magnetic stainless steel.

A more feasible choice was Inconel 600. This material has a CTE of 6.5 in/in/°F. The magnetic permeability is 1.005 in cgs units. A sample lot of this material was purchased and end shields were being fabricated to evaluate a stator assembly. The axial stresses in the slot bridge will be reduced to less than 10,000 psi and the radial stress to under 6000 psi.

Two stator assemblies were fabricated for evaluation with the following changes from the original configuration:

- Inconel 600 end shields
- No epoxy backfill between potted stator windings and end shields.

These assemblies were processed in accordance with normal stator assembly sequence, i. e. ;

- Grind OD to within 0.0004 inch of correct size
- Temperature cycle to 300°F
- Grind to final size

Roundness was measured at all stages of processing. These results, along with the readings after sterilization cycling, are shown in Table 11.

Table 11. Slot Bridge Concentricities

Processing Stage	Unit No. 1			Unit No. 2		
	Top	Middle	Bcttom	Top	Middle	Bottom
Initial Grind	20	25	50	30	20	25
1 st Temperature Cycle	200	300	400	110	50	120
Final Grind	25	30	30	25	30	30
1 st Sterilization Cycle	150	175	175	160	160	350
3 rd Sterilization Cycle	150	175	175	160	170	350
6 th Sterilization Cycle	180	175	190	180	150	350

NOTE: All readings in microinches

These results show that the slot bridge will assume a stable position after the first sterilization cycle.

In addition to measuring roundness, size was measured to determine if slot bridges were deforming as they did on the unit that failed. The diameter on unit No. 1 was uniform within 40 microinches and within 60 microinches on unit No. 2. The corresponding readings on the original assembly were 800 to 1000 microinches. This indicates that the basic problem is solved.

Based on testing and analysis, the following procedure was used on the rebuild of the sterilization gyro:

- (1) Use of new configuration Inconel 600 end shields
- (2) Eliminate the epoxy backfill, retain an epoxy insulation on the inside of the end shield
- (3) Modify the processing sequence as follows:
 - Grind slot bridge to within 0.0008 inch of correct size
 - Temperature cycle to 300°F
 - Grind slot bridge to within 0.0004 inch of correct size*
 - Run one sterilization cycle*
 - Grind slot bridge to the correct size
 - Run three sterilization cycles on the assembly
 - Re-inspect the assembly*
 - Assemble and check out motor
 - Run three sterilization cycles on completed spinmotor and gimbal assembly
 - Continue into normal gyro build

*Denotes changes from previous processing sequence.

After the first rebuild of the gyro was complete, the performance of the unit was erratic. The gyro was disassembled and a teardown analysis was conducted on the unit. The cause of the erratic performance was traced to a dielectric failure in the pump.

The pump assembly was carefully disassembled to determine the exact cause of the failure. The breakdown was traced to a weak insulating area between the stator windings and the inner stator. The area of the failure is shown in Figure 11. The breakdown occurred at the corner radius of the stator.

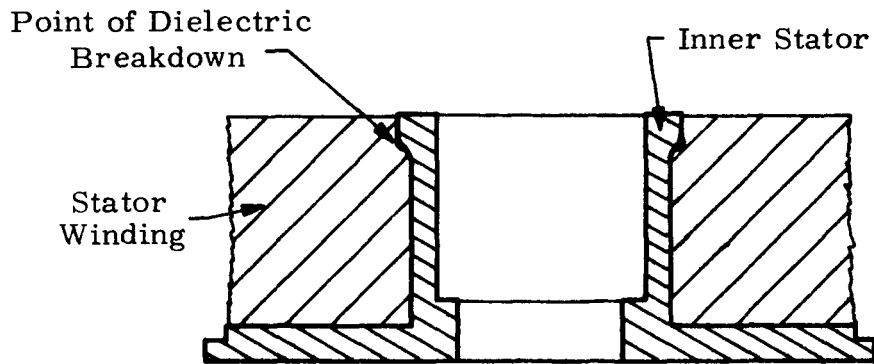


Figure 11. Cross-Section View of Pump Stator and Windings

A new pump assembly was built with special care being taken to assure that the inner stator was adequately insulated.

SECTION VII FINAL TEST RESULTS

Testing on the gyro consisted of the following:

- Initial checkout and trim
- Random drift
- Runup to runup stability
- Vibration
- Five sterilization cycles

CALIBRATION AND ADJUSTMENTS PRIOR TO INITIAL TESTS

The resistance of the temperature sensing element was checked by placing the gyro in a 185°F water bath. The sensor was then series padded to 780 ohms at 185°F.

The fixed torques were compensated to -0.13 deg/hr with a pump frequency of 20 cps.

The mass unbalance terms were compensated to 0.16 deg/hr along the IA and 0.57 deg/hr along the SRA.

TEST RESULTS

Vibration

The gyro was vibrated and the anisoelastic coefficient was determined during the initial tests, after the first and fifth sterilization cycle. The results of

the tests are shown in Figures 12, 13, and 14. The attitude angle coefficient was determined during the initial test and results are shown in Figure 12.

Stability and Random Drift

The g-sensitive and non-g-sensitive torques were determined initially and after each sterilization cycle. A complete balance torque history is shown in Figure 15. Table 12 lists the torque shifts and the random drift after each sterilization cycle.

The torque shifts during sterilization cycling are not excessive except for the first cycle. It is normal for a gyro to shift during the first temperature cycling after final build. This shift could be eliminated by an initial temperature cycle before trimming and proceeding to the sterilization cycling.

The OAV runup to runup stability of the unit was measured initially and after the fifth sterilization cycle. The results, tabulated below, are well below the requirement of 0.02 deg/hr maximum.

Initial - 0.011 deg/hr (RMS Dr, 5 cycles)
First Cycle - 0.007 deg/hr (RMS Dr, 5 cycles)
Fifth Cycle - 0.00 deg/hr

The various gyro parameters are listed in Table 13.

Figure 16 is an installation drawing with outline dimensions.

The circuit schematic is shown in Figure 17.

The excitations for the various circuits are given in Table 14.

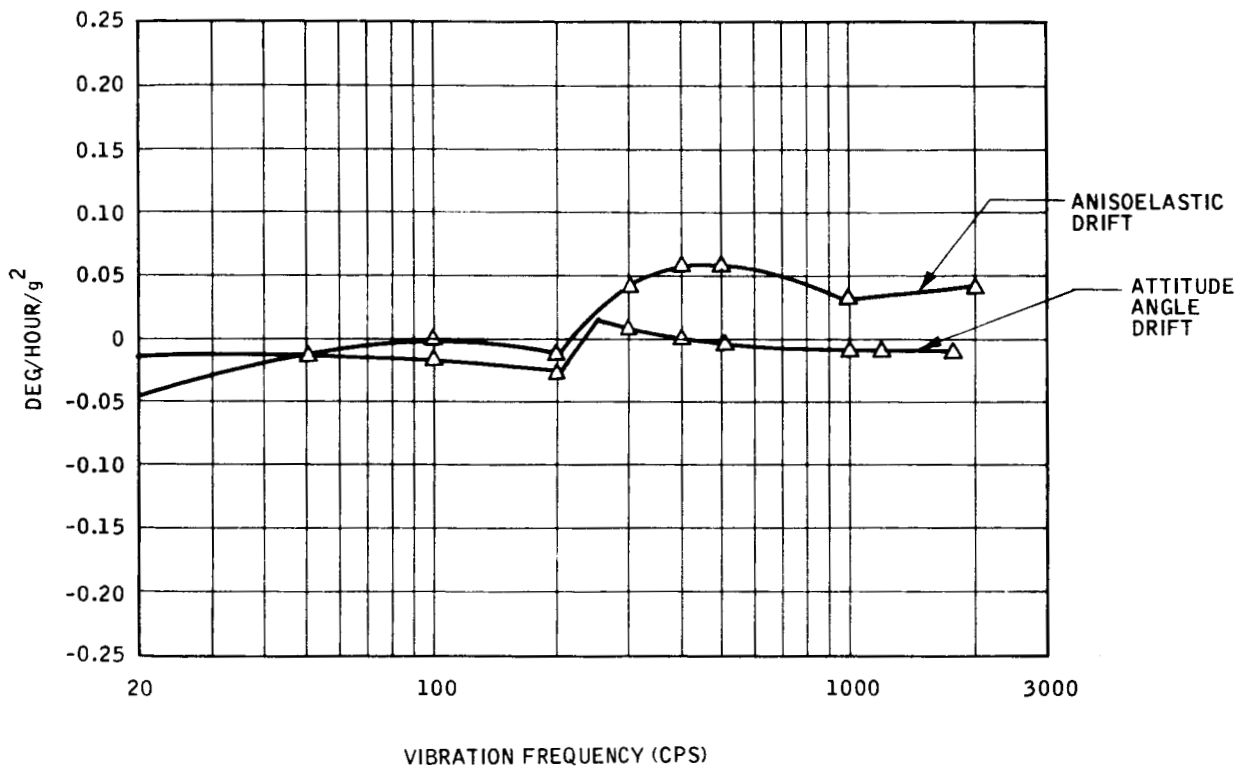


Figure 12. Attitude and Anisoelastic Drift Coefficient 5 g RMS

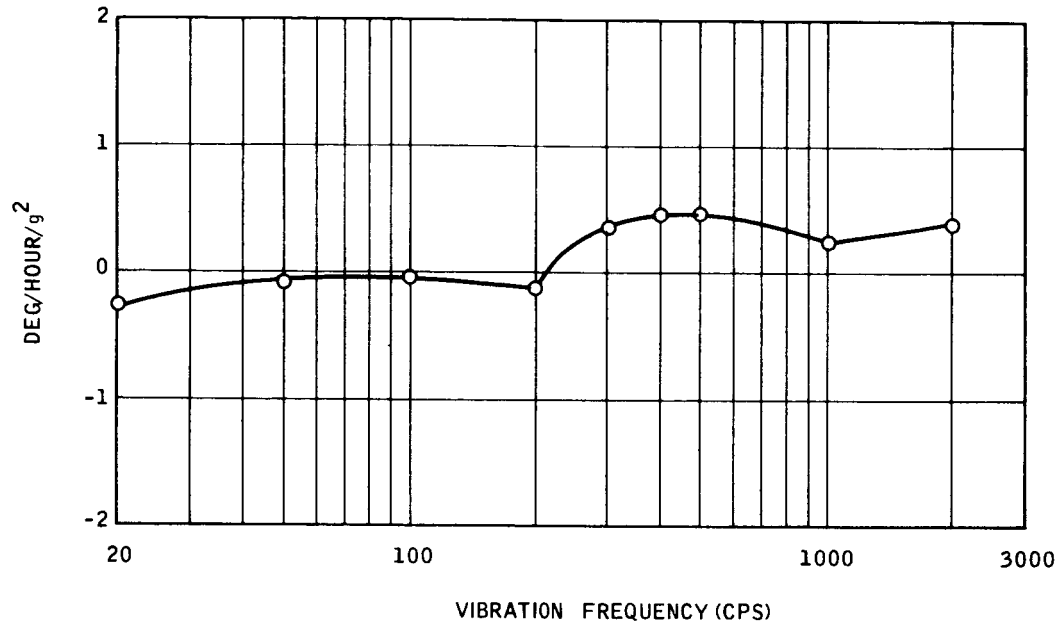


Figure 13. Anisoelastic Drift 5 g RMS Post +300°F Cycle No. 1

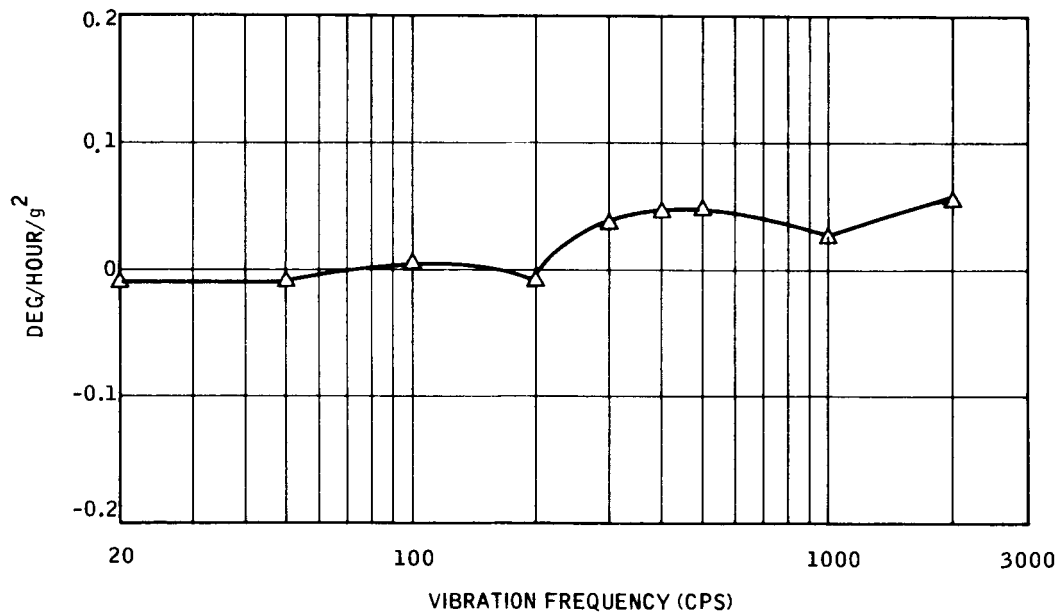


Figure 14. Anisoelastic Drift Coefficient Post +300°F Cycle No. 5

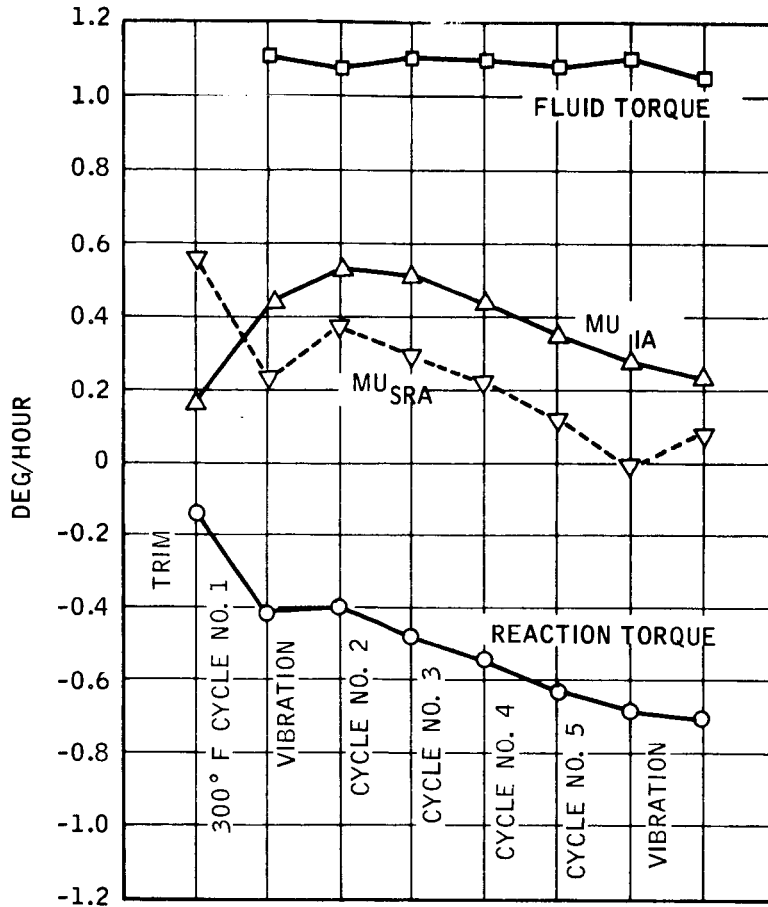


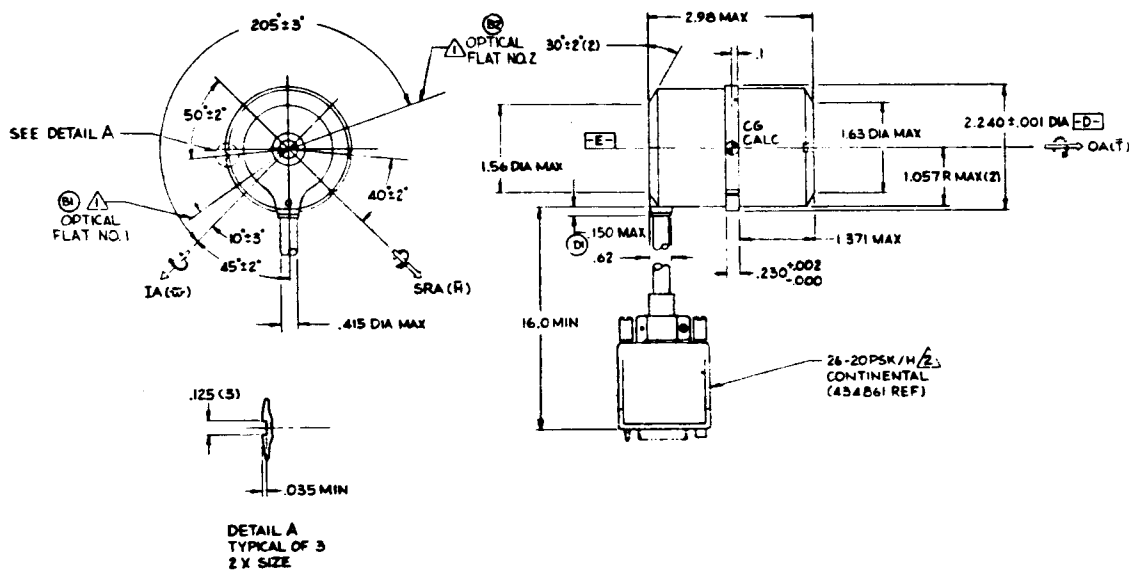
Figure 15. Gyro Balance Torque History

Table 12. Torque Shifts and Random Drift

Cycle Number	Torque Shifts (deg/hr)			Random Drift deg/hr 4 hr, 1 σ		Drift Trend (deg/hr/hr)	
	RT	MU _{IA}	MU _{SRA}	OAV	IAV	OAV	IAV
Reference	---	---	---	0.003	0.002	0.0002	0.0007
1	-0.26	0.26	-0.34	0.003	0.002	-0.0007	-0.0004
2	-0.07	-0.02	-0.09	0.001	0.001	0.0002	-0.0002
3	-0.07	-0.08	-0.07	0.001	0.002	-0.0005	-0.0010
4	-0.09	-0.08	-0.10	0.001	0.002	-0.0005	-0.0009
5	-0.04	-0.08	-0.13	0.002	0.003	0.0008	-0.0013

Table 13. Gyro Characteristics

Gyro Transfer Function	234 mv/mr
Damping	9,700 dcm-sec/rad
Signal Generator Sensitivity	23.7 mv/mr
Torque Generator Sensitivity	90.0 deg/hr/ma
Gimbal Freedom	1.52 deg
	-1.51 deg
Elastic Restraint	-0.038 deg/hr/mr
Signal Generator Null Voltage	1.5 mv



⊕ DATUM E IS THRU ACTUAL CENTER OF DATUM D
 ⊕ MATING CONNECTOR CONTINENTAL 26-2055 REF
 ⊕ GYRO ALIGNMENT MIRROR LOCATION

Figure 16. GG159 Gyro Outline Dimensions

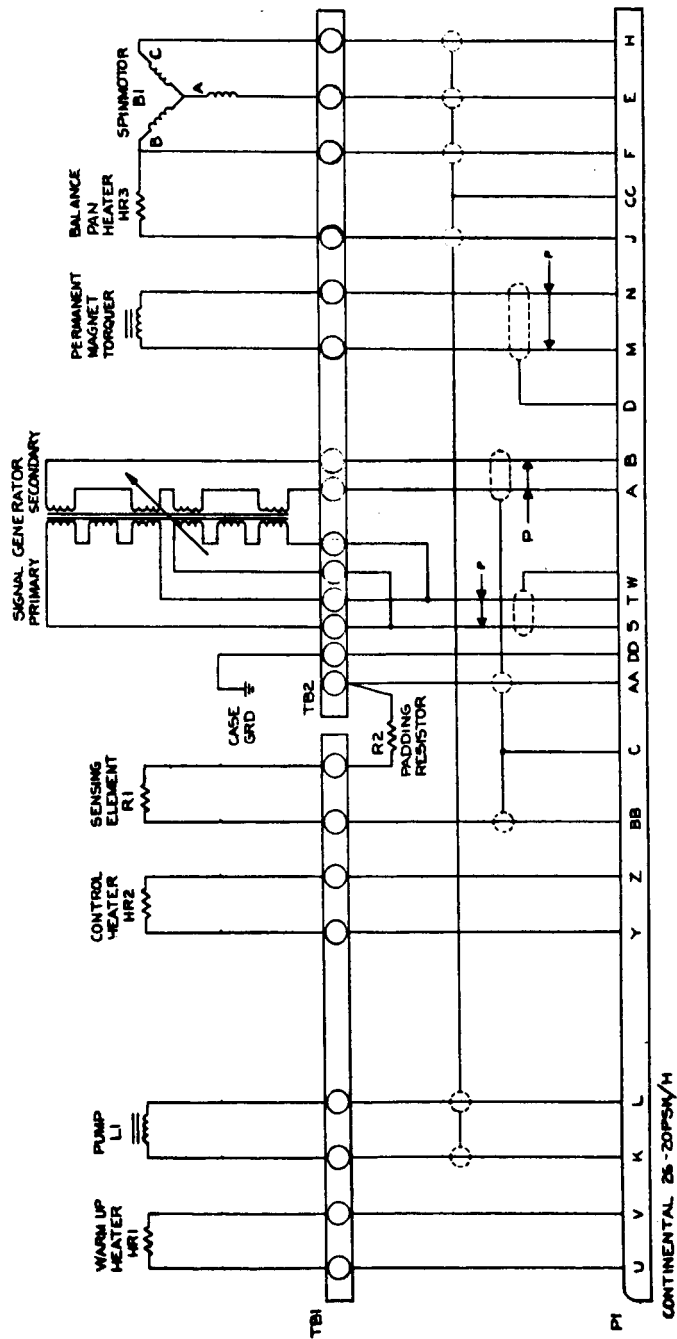


Figure 17. GG159 Gyro Schematic Diagram

Table 14. Power Supply Requirements

Circuit	Magnitude	Tolerance Percent	Stability While Applied in Percent	Source Impedance Ohms
Sensor Excitation				
Volts (ac or dc)	10.0	Max		
Heater Supply (Proportional Control)				
Heater Warm-up				
Volts (ac or dc)	120	Max		
Watts	55	Max		
Heater, Control				
Volts (ac or dc)	32	Max		
Watts	7.3	Max		
Hydrostatic Pump				
A. Volts ac rms	30		0.2	
Watts	2.0	Max		
Frequency	20 cps	1.0	0.2	
B. Volts (peak dc)	31		0.2	
Watts	2.0	Max		
Frequency	25 cps	1.0	0.2	
Duty cycle	25%			
S. G. Primary Excitation				
Volts	10.5	±2	±1.0	Less than 100 at 7.2 kc
Watts	0.8			
Frequency	7200 cps	±0.1		
Harmonics	2%	Max		
Spin Motor Excitation				
Sinusoidal - 3-phase.				
Frequency	800 cps	±0.01		Less than 4 + j4 line-to-line at 800 cps
Volts (φ - φ): Run	36v	+1v, -0v	±0.10	
Start	50v	+5v, -0v		
Current/(φ) Start	400 ma			
Current/(φ) Run	190 ma			
Watts (total) Start	20			
Watts (total) Run	6.0			
Harmonics	3%	Max		
Torquer Generator				
Current Range (continuous dc)	0-100 ma	Max		
Watts	1.0	Max		

SPINMOTOR PERFORMANCE

The spinmotor performance characteristics did not change during the sterilization cycling. Starting voltages before and after the complete testing are tabulated below.

	<u>Starting Voltage (May)</u>	
	<u>Journal</u>	<u>Thrust</u>
Initial	29.5	36
Final	29	37

An abnormal spinmotor condition was discovered when the motor was turned off with the gyro at operating temperature. The motor would not synchronize with up to 50 volts/phase of applied excitation. This condition was discovered very shortly after the gyro was in test.

An investigation was conducted to determine the exact spinmotor performance before proceeding with further testing.

The history of the unit up to this point showed nothing to indicate a problem. The last check at the gimbal level before proceeding into gyro build showed a minimum sync voltage of 36.5 volts per phase and starting voltages of 30-33 volts per phase.

After the first rebuild, before the pump failure, no abnormal spinmotor conditions were noted. The gyro was torn down and no further checks were made on the spinmotor until the second rebuild was completed. It is possible that the spinmotor was damaged during the machining operation to open the case.

The spinmotor testing revealed the following. At room temperature the spinmotor will synchronize with 42-48 volts. If the voltage is reduced to 36 volts per phase, the spinmotor will continue to run at synchronous speed. (This procedure was used during all of the subsequent testing.)

Table 15 summarizes the synchronous operation characteristics.

Table 15. Synchronous Speed Characteristics

Temperature	Before Temperature Cycling		After 5 Sterilization Cycles	
	Sync Voltage	Method	Sync Voltage	Method
40°F	42-50	Normal		
70°F	43-48	Normal	43-48	Normal
100°F	45-48	Normal	44-47	Normal
135°F		Runup at 48v, Reduce quickly to 36v	--	Runup at 48v, Reduce quickly to 36v

Above 160°F Motor will not reach synchronous speed

From 130°F to 160°F, the spinmotor will not reach synchronous speed with 48 volts per phase. The motor is slipping from synchronous speed at a very slow rate. If the voltage is decreased rapidly, less than one second, to 36 V/φ, the spinmotor will lock in at synchronous speed. Above 160°F it was not possible to bring the motor up to synchronous speed.